November-December 2019
ISSN: 0193-4120 Page No. 5137 - 5145

Efficient Log-based Iris Detection and Image Sharpness Enhancement (*l*-IDISE) using Artificial Neural Network

S. Venkata Lakshmi, K. Sathyamoorthy, *K. Sujatha, Ashish Kr. Luhach
Panimalar Institute of Technology, India
Wenzhou-Kean University, China
The PNG University of Technology, Papua New Guinea
Corresponding author: sujatha.ssps@gmail.com

Article Info
Volume 81
Page Number: 5137 - 5145
Publication Issue:
November-December 2019

Abstract

Identification of people managed by Biometric, and it is dependent on their organic qualities. Iris Recognition System (IRS) is viewed as the most dependable and exact biometric recognizable proof framework accessible. Conventional individual validation techniques have numerous intuitive imperfections. Biometrics is a compelling innovation to conquer these imperfections. Biometric oversees the Identification of individuals subject to their natural properties. Iris Recognition System (IRS) is seen as the most reliable and exact biometric unmistakable verification structure available. Standard individual approval methodologies have various instinctual methods. Biometrics is a reasonable advancement to overcome these distortions. In this paper, a methodology for IRS has proposed systems for developing and to distinguish the pupil. The noises, for example, eyelashes, and reflections are expelled through the straight thresholding. The 3D log is applied for highlight extraction from a fragmented iris image (IMG).It is seen that the proposed methodology is increasingly proficient for the considered dataset from the test results. It is likewise seen that the proposed methodology sets aside sensible measures of effort to perform iris division, and acknowledgment precision is additionally sensible. Hazy, little resolution IMGwith poor light make a significant test for IRS are the examples for Low-quality iris IMG. This proposed l-IDISE is planned to structure an IRS in three first strides to confirm the objective. (1) Applying IMG handling procedures on the image of an eye for information arrangement. (2) The Back Propagation Artificial Neural Network (BPANN) systems for recognizable proof. Third new IRS calculation for improvement of standardized iris IMG. The Logarithmic Image Processing (LIP) IMG upgrades process. Consequences of numerous biometric stupendous test iris information show noteworthy improvement in the presentation of IR calculations as far as equivalent mistake rates. The BPANN was prevailing in recognizable proof and getting the best outcomes since it achieved Recognition Rate equivalent to 90%.

Article History

Article Received: *5 March 2019*
Revised: *18 May 2019*
Accepted: *24 September 2019*
Publication: *24 December 2019*

Keywords: *Iris Recognition System, Image Processing, Artificial Neural Network, Patten Matching, Iris Detection well-being; gen y*

1. Introduction

A few biometric procedures were utilized for distinguishing proof of people from the previous century. These strategies are Iris Recognition (IR) [1], Face acknowledgment, Fingerprint acknowledgment, Voice acknowledgment, and so forth. Every one of these strategies has many authenticated applications. IR alludes to the digital strategy for confirming a match between two irises of humans [2].Irises are one of the numerous types of

November-December 2019
ISSN: 0193-4120 Page No. 5137 - 5145

biometrics used to distinguish people and check their character. IMG quality is a significant factor in the presentation of an IRS. At the point when the more excellent IMGis not accessible, the IR can be undermined by utilizing the low-quality IMG, for example, those procured in a non-intrusive, non-helpful condition, for example, iris IMG got a good ways off and progressing. These IMG described by active corrupting components, for example, low goals, lighting and complexity, broad specular reflections, eyelid impediment, nearness of contact focal points and diverting eye product, and so on. Along these lines, strategies for iris IMG improvement have a significant impact on adding to the exactness of the IRS.

The fundamental focal point of this task is to create a biometrics IRS. It recognizes individuals by breaking down examples of their irises, which are professed to be one of a kind for each person and stable over extensive periods. The general structure of irises is resolved hereditarily while little subtleties rely upon external variables, for example, starting states of the fetus advancement. In this way, it is profoundly improbable for two irises to be framed in thesame manner. They are remarkable to individuals and stable with age. The distinction even exists between indistinguishable twins and between the left and the right eye of a similar individual.

The objective is too accomplished through after advances. (1) By applying Image Processing (IP) methods for explaining iris IMGnecessary for separating information by utilizing iris: obtaining, limitation, upgrade, and division. (2) Propose another quick and compelling iris IMG improvement calculation dependent on logarithmic IMG, preparing for upgrades sharpness and the light of anIMG.The third is the proposed LIP-based calculation appeared at a 5% improvement in the check rates when contrasted with the other quick strategies for the IMGupgrade. (3) Involves Neural Network systems for correlation and distinguishing proof, which spotlights on Back Propagation Artificial Neural Network (BPANN).

2. Related Works

The most dependable biometric framework is the Irisrecognition system because of the one kind arbitrary highlight of an iris. Different creators proposed distinctive iris acknowledgment framework since after the Daugman grew first business iris acknowledgment framework. Daugman's [3] calculation received 2D Gabor channels to demodulate the iris stage data and concentrate highlights.

A 1-D dyadic wavelet conversionutilizingiris acknowledgment framework with different goals levels on an iris IMG to describe the surface of the iris and after that utilized zero-intersection for highlight portrayal. It utilized two uniqueness capacities to contrast the new example and the reference designs. Boles‟ methodologies have the upside of preparing 1-D iris flag as opposed to a 2-D [4]IMG. Here, "1D dyadic" signifies a couple of 1-dimensional wavelet channels, for example, low pass and high pass channels.
The utilization of the 2D stage congruency to extricate the iris highlight. The technique performed well even within sight of noise because of individual enlightenment or other variation conditions. The stage congruency characterized in terms of the Fourier arrangement extension of a sign inthe area. A biometric framework is an example acknowledgment framework that perceives an individual based on an element vector obtained from a particular physiological or conduct trademark that the individual has.

Ophthalmologists Alphonse Bertillon and Frank Burch were one among the first to recommend that iris examples can be utilized for distinguishing proof frameworks. In 1992 [5], John Daugman was the first to build up the iris distinguishing proof programming. An iris acknowledgment calculation was dependent on LPCC and LDA. What's more, they presented a straightforward and quick preparing calculation, molecule swarm enhancement, for preparing the Probabilistic Neural Network.

New calculations for iris division, quality upgrade, coordinate score combination, and order to improve both the exactness and the speed of iris acknowledgment. A curve advancement approach is proposed to effectively segment a no perfect iris IMG utilizing the changed Mumford–Shah utilitarian [6]. Distinctive upgrade calculations are simultaneously applied to the fragmented iris IMG to deliver numerous improved renditions of the iris IMG [7].

3. Design and Implementation

3.1 Image Acquisition

The initial step for any IRS is by securing an iris IMG. Because of the diminutive size of an iris, around 11 mm in breadth, makes the iris procurement troublesome. IMGacquisitions assume a significant job in the IR. For the present undertaking, eye assistance association, iris IMG database has been utilized.This iris IMG database mostly comprises of the iris IMG gathered from an Image database. The gained IMG was spared in the bitmap group. The database of 500 IMG is procured from 500 distinct clients and made accessible openly to the scientists. Every one of the subjects in the database is in the age team 25 - 35 years, including 300 guys and 200 females. The goals of these IMG are 320 x 240 pixels, and every one of these IMGwas obtained in the indoor condition [8].

3.2 Segmentation

Separating the iris area from the given eye IMG, which is to be utilized for isolating reason is Segmentation. In this present task work, Algorithm 1 and Algorithm 2 have

November-December 2019
ISSN: 0193-4120 Page No. 5137 - 5145

been executed to distinguish the iris inward (pupil Detection) and external limits (iris Detection) separately [9].

3.2.1 Algorithm for Eye Pupil Recognition

Input: Test Human Eye Image

Output : Image Pupil Centre =PC_x,PC_yandradius =PC_r

Step 1: Generate the Binary image of the input eye image by linearthresholdingtechnique.

Step 2: Perform median filtering and morphological operations on the binaryimage

Step 3: Calculate the centroid of the pupil area(PC_x, PC_y) by using sectionattributes.

Step 4: For determining the radius of the pupil PC_r

- Count the number of 1‟s present on the HL- Centroid to the left
- Count the number of 1‟s present on the VL - Centroid to the top,(i.e.)PC_{ry}.
- Computing the average of $PC_{rx}$and PC_{ry}.$PC_r = PC_{rx} + PC_{ry}/ 2$

Step 5: Centroid (PC_x, PC_y) and Radius PC_r, segment the pupilstate from the eye image.

3.2.2.Algorithm for Iris Finding

Input: Eye image with detected pupil region,(PC_x, PC_y)

Output: Iris center(PC_x, PC_y), radiusPC_i

Step 1: Select two rectangle of small sizefrom both side of the detected pupil.

Step 2: Perform canny edge detection method to detect the vertical line the center point of each of the line,

- $PC_1(PC_{X1}, PC_{Y1})$ and $PC_2(PC_{X2}, PC_{Y2})$.

Step 3: estimate the distance DP_1 and DP_2 of the point DP_1 and $DP_2$from thecenter(PC_x, PC_y)

$$DP_1 = \sqrt{(PC_x - X)^2 + (PC_x - Y_1)^2} \quad \ldots\ldots\ldots\ldots\ldots\ldots\ldots\ldots\ldots\ldots(1)$$

$$DP_2 = \sqrt{(PC_x - X)^2 + (PC_x - Y_2)^2} \quad \ldots\ldots\ldots\ldots\ldots\ldots\ldots\ldots\ldots\ldots(2)$$

Step 4: The radius of the iris isthe average of the distance $DP_1$and DP_2

$$PC_r = \frac{DP_1 + DP_2}{2} \quad \ldots\ldots\ldots\ldots\ldots\ldots\ldots\ldots\ldots\ldots(3)$$

Step 5: Centroid(PC_x, PC_y)and radius PC_r,segment the iris area.

3.3Normalization

Recognized around iris locale is changed over to the rectangular state of uniform size in the standardization step. For this reason,Daugman‟s Rubber sheet model (refer figure 1) has been utilized. The rubber sheet model considers the dilation ofpupil model remaps each point inside the iris district to a couple of polar directions (PC_r ,θ)where $PC_r$is on the interval [0,1], and θ is angle [0,2π].

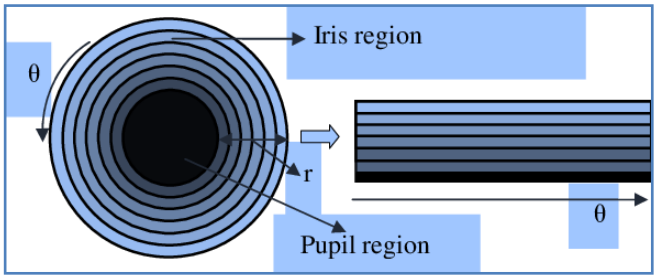

Figure 1: Daugman‟srubber sheet representation

The (PC_x, PC_y) Cartesian directions to the standardized non-concentric polar representation for the remapping of the iris locale is displayed as :

$$iR = (PC_x(PC_r,\theta),(PC_y(PC_r,\theta)) \rightarrow iR(PC_r,\theta) \quad \ldots\ldots\ldots\ldots\ldots\ldots\ldots\ldots(4)$$

$$PC_x(PC_r,\theta) = (1-PC_r)X_p(\theta) + PC_{rx1}(\theta) \quad \ldots\ldots\ldots\ldots\ldots\ldots\ldots\ldots\ldots\ldots(5)$$

$$PC_y(PC_r,\theta) = (1-PC_r)Y_p(\theta) + PC_{ry1}(\theta) \quad \ldots\ldots\ldots\ldots\ldots\ldots\ldots\ldots\ldots\ldots(6)$$

(PC_x, PC_y) are the first Cartesian directions, (PC_r,θ) is the comparing standardized polar coordinates and are the directions of the student and iris limits along the θ coursewhere, I(PC_x, PC_y)is the iris environment representation. The elastic sheet model considers pupil dilation and size irregularities to create a standardized portrayal with consistent measurements.By looking at the IMGdatabase, it is discovered that more often than a not upper piece of the recognized iris is covered by the top eyelid. In this way, just left, the right, and base side of recognized iris, for example, the range edge θ from PC_i – PCi/8 to 2 ∗PCi + PCi/8, is considered as a standardized iris format which is to be utilized for verification reason as appeared in the figure. 2.

November-December 2019
ISSN: 0193-4120 Page No. 5137 - 5145

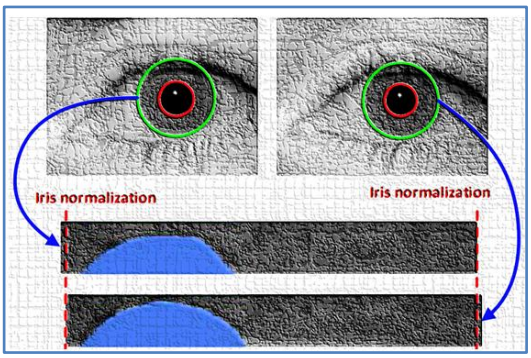

Figure 2. Iris Normalizing Form

3.4 Noise Detection

For example, eyelashes, specular reflections may show in the standardized iris format for the detection of noise. A direct thresholding procedure has been utilizedto disconnect these noises. The region with pixel esteem under 30 is considered as an eyelash, and the pixel esteem more noteworthy than 241 is considered as reflection. The mask called noise cover is made with the restricted commotions present in the standardized iris. The pixel with the result of the noise recognition step has appeared in figure3.

Figure 3. Noise Mask Iris

3.5 Feature Extraction

To separate the unique highlights from the standardized iris layout, the 3D log has been applied. The 3D standardized example is separated into the various 3D flag and convolved with 3D. The lines of the standardized example are taken as the 3D signal; each line relates to a rounded ring on the iris locale.

3.6 Iris Matching

For coordinating reason, the Hamming separation with the consolidation of noise covering was utilized as acknowledgment metric, so just critical bits are utilized in computing the Hamming separation between two iris formats. Presently when taking the Hamming separation, just those bits in the iris design that compares to "0" bits in noise masks of both iris examples will be utilized in the figuring. The Hamming separation will be determined to utilize just the bits produced from the genuine iris locale, and Hamming separation recipe is given as

$$H_D = \frac{1}{n - \sum_{k=1}^{n} X_{nk} \otimes Y_{nk}} \sum_{j=1}^{n} X_j (\otimes) Y_j (\oplus) X_{n_j'} (\oplus) Y_{n_j'}$$

Where,$X_j$and $Y_j$are the two bit-wise patterns to evaluate, $X_{nj}$and $Y_{nj}$are theequivalent noise mask for X_j,and $Y_j$and N is the number of bits symbolized byeach template.

4. Proposed *l*og-Image Enhancement Algorithm (*l*-IEA)

This work utilized the IMG improvement technique proposed on ***l*-IEA** applied to the system of Lee's IMGupgrade calculation. This new usage of Lee's calculation indicated a high capacity to build the general differentiation and the sharpness of anIMG. The ***l*-IEA** is depicted as pursues.To start with, IMGmagnitude work is changed over to the gray tone work, *f*: F (*p*,*q*) = Mg - *f*(*p*,*q*), where Mg=256 for an 8-piece representation. The gray tone work, thus, is changed to the standardized negative gray tone work employing: This is known as a standardized supplement change [10] [11].

$$\bar{f} = 1 - \frac{f}{Mg}$$

Next, the log of the standardized negative gray tone capacity:

$$\log(\bar{f}(p,q)) = \alpha \log(\bar{\partial}(p,q) + \beta[\log(\bar{f}(p,q)) - \log(\bar{\partial}(p,q)]$$

Where is the mean estimation of in a ($\eta_x\eta$) window focused at (p,q). Upgraded yield IMG F' is gotten by changing over back to the first scale.

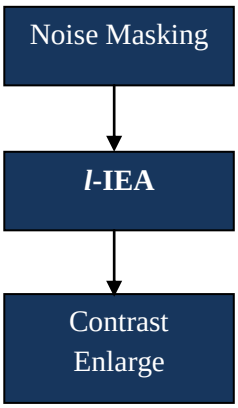

Figure 4. Proposed l-IEA flow

The calculation is constrained by three parameters: α, β, and η. The first parameter, α, is

November-December 2019
ISSN: 0193-4120 Page No. 5137 - 5145

utilized to adjust the dynamic scope of anIMG: the dynamic scope of the dull (splendid) zones of anIMG is extended when α<1 (α>1). The littler the worth α, the more splendid the IMG will show up.The sharpness of anIMG is controlled with parameter β Є [0,255] like that of the unsharp covering: more exceptional qualities lead to the more sharpenedIMG, even though the noise pixels will likewise be nonlinearly intensified. When β =1, the sharpness of the IMG doesn't change [12].

The proposed iris IMG improvement calculation included *l*-IEA included noise covering other l-IEA applications and resulting complexity extending. The accompanying info parameters were chosen to be applied to the standardized iris IMG: α = 0.7, sharpness β =2, η =3. Now we didn't separate between the individual IMG properties to modify these parameters. The choice of these parameters was performed utilizing visual inclinations of the presence of the most iris IMG in the dataset. Complexity extending (0.0-1.0) was applied to the ***l*-IEA**prepared IMG to build differentiate.The decision of these parameters was performed using visual tendencies of the nearness of the most iris IMG in the dataset. Contrast broadening (0.0,1.0) was applied to the ***l*-IEA** arranged IMG to extend separate.At some stage in this progression,the noisy pieces of the IMG will, in general, take up the most noteworthy dark scale esteems, with the goal that the most significant part of the IMG still stays in low complexity. To stay away from this trap, the noisy piece of anIMG was concealing with the mean grayscale [13] estimation of the remainder of the IMG preceding ***l*-IEA**and histogram extending.The case of an upgraded IMG utilizing diverse rendition of the ***l*-IEA**has appeared in the figure. 5. The proposed ***l*-IEA** calculation was applied to the standardized iris IMG of size 128x720. After the improvement,IMG was cut back to 20x240 before encoding. Cutting back diminished the noise delivered by ***l*-IEA** and stressed the most important details. Utilization of the ***l*-IEA**: noise is covered with the standardgray worth, ***l*-IEA** is applied with parameter esteem a=0.7, completed with differentiation extending (0.0, 1.0).

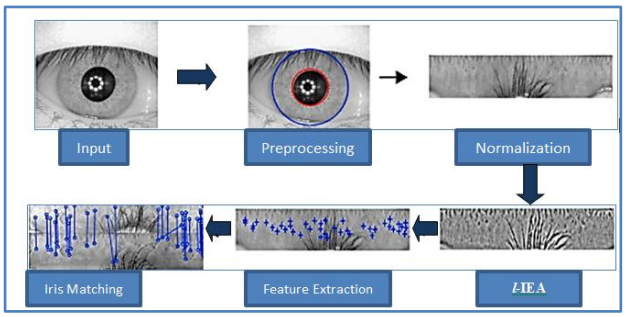

Figure 5. Image pattern conversion and matching

4.1. Back Propagation Artificial Neural Network (BPANN)

The PCs whose engineering is designed according to the mind by BPANN. They ordinarily comprise a considerable number of basic handling units, which wired together in an unpredictable correspondence arrange. Every unit or hub is a rearranged model of a genuine neuron, which fires (sends off another sign) if it gets an adequately reliable info signal from different hubs to which it is associated. The quality of these associations might have fluctuated to perform various undertakings relating to various examples of hub terminating movement. The exhibition of the constraints of single-layer neural systems was a noteworthy factor in the decrease of enthusiasm for neural systems. The BPANN was made by summing up the Windrow-H off learning guideline to various layer systems and nonlinear differentiable initiation capacities. Appropriately prepared BPANN [14] will, in general, offer sensible responses when given sources of info that they have never observed. Commonly, information prompts a yield like the right yield for info vectors utilized in preparing that are like the new information being displayed. This speculation property makes it conceivable to prepare a system on a delegate set of info/target combines and get excellent outcomes without preparing the system on all conceivable information/yield sets.The preparation of a system by Back Propagation includes three phases: the feedforward of the info preparing a design, the count and Back Propagation of the related blunder, and the change of the feed-forward stage. Regardless of whether preparing is moderate; a prepared net can create its yield quickly. More than one shrouded layer might be advantageous for specific applications; however, one concealed layer is adequate for general purposes.

4.2. Algorithm of BPNN

a) The feed-forward [15] of the information preparing design, the BPANN of the related mistake, and the modification of the loads. During feedforward, each

November-December 2019
ISSN: 0193-4120 Page No. 5137 - 5145

information unit (X*i*) gets an info sign and communicates this sign to every one of the concealed units Z_1 ….. Z*p*through the (v) loads. Each concealed unit at that point figures its initiation and results in its sign (Z_j) to each yield unit through the (w) loads. Each yield unit (Y*k*) registers its actuation (Y*k*) to frame the reaction of the net for the given info design. During preparing, each yield unit contrasts its figured actuation Y_k and its actual worth T_k to decide the related mistake for that example with that unit.

b) Based on this mistake, the factor k (k=1 … m) is registered, k is utilized to disperse the blunder at yield unit Y_k back to all units in the past layer (the concealed units that are associated with Y_k). It is likewise utilized (later) to refresh the loads between the yield and the concealed layer.

c) Approximately, the factor j (j=1 … .. p) is figured for each concealed unit Z_j. It isn't vital to disseminate the blunder back to the info layer, yet j is utilized to refresh the loads between the concealed layer and the information layer. At the point when every one of the variables has been resolved, the loads for all layers are balanced all the while.

d) The change following the weight W_{jk} (from shrouded unit Z_j to yield unit Y_k) depends on the factor K and the actuation $Z_j$of the concealed unit Z_j. The change per the weight V_{ij} from info unit X_i to concealed unit Z_j) depends on the factor j and the initiation X_i of the information unit. Age is one push through the whole arrangement of preparing vectors. Commonly, various ages are required for preparing a BPANN. The prior calculation refreshes the loads after each preparation example is introduced. A typical variety is a clump refreshing, in which weight updates are amassed over a whole age before being applied.

5. Result and Discussion

5.1. IR SampleDataset

Table 1: Information about the images in the database

Image Extension	BMP
Image co-ordination	640x480
$Image_W$	640 pixels
$Image_H$	480 pixels
$Imgae_{Size}$	350 kb
Image Colors	Gray Scale

This work applied our IMG upgrade calculation to standardized iris IMG acquired from the MBGC information. Display IMG originated from iris video, and test IMG was taken from the face recordings. For the acknowledgment procedure, just one IMG was chosen from every video grouping. The model IMGhas appeared in Figure 6. The comparing iris IMG was edited from the keenest edge in each face video arrangement. Iris video and face video IMGgave by and large 220 and 120 *pixels* over the iris. Video iris IMGdisplayed low complexity; however,it demonstrated sensible sharpness.The most laborious information was spoken to by the iris IMGedited from face recordings: they were portrayed by low brightening and complexity, low goals, meddling specular reflections. Information was assembled in four examinations: Left 1: Left 2; Right 1 Right 2. The size of exhibitions and tests for the examinations extended 69-72 and 139-140 IMGseparately(refer table 1).

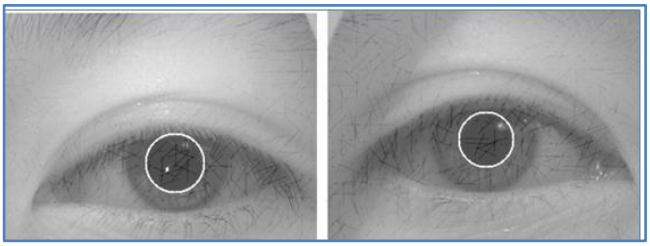

Figure 6. Iris sharpness test result

5.2. Iris SegmentationResults

The proposed methodology division results on various eye IMGhave appeared in figure7. The regular time to disconnect iris from an eye IMG is about 1.08 *sec*.

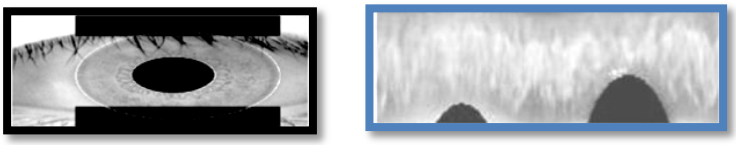

Figure 7. Segmented and Normalization Iris

To assess the exhibition of the proposed methodology, the outcomes got by the proposed methodology for iris division. The outcomes were classified in table 2.

Table 2: Iris segmentation results

TechniqueUsed	Successive Time of IR
• Pupil limitation by basic morphological tasks. • Eyelashes and reflections are removed	1.014

November-December 2019
ISSN: 0193-4120 Page No. 5137 - 5145

bylinear thresholding. • Direct thresholding is evacuated by eyelashes and reflections. • Iris span is determined by point choosing focuses on the iris fringe	

5.3. Result of Iris Recognition

The Humming Distance [16] is embraced as the measurement of uniqueness between information iris layout and selected iris formats for acknowledgment reason. The presentation of IR is evaluated with acknowledgment exactness determined as

$$\Pr ecision = \frac{TotalNo.ofTimeSpersons\,\mathrm{Re}\,cognises}{TotalNo.of\ \mathrm{Re}\,cognization} x100$$

The average recognition accuracy is obtained as 98.17% from the experimental results.

Table 3: Accuracy Results

Techniques	Outcome
Existing Method	96.13 %
Proposed *l*-IDISE	98.17 %

It thought about the consequences of IR execution utilizing our iris IMG improvement and other mainstream existing methodologies: histogram equalization, unsharp concealing, homomorphic separating actualized, and foundation subtraction. The choice of the iris IMG upgrade calculations for results examination was based utilizing the model of the quickest runtime (inside 1.01*sec*. utilizing MATLAB).Various adaptations of the use of ***l*-IEA** upgrade: unique ***l*-IEA, *l*-IEA** with difference extending, masking pursued by to***l*-IEA**, were likewise incorporated into the investigation to legitimize the need of three phases in the proposed calculation. We applied these iris IMG improvement calculations to be utilized with a similar iris division, standardization, commotion veiling, and highlight encoding calculations.The division was performed dependent on our entropy-based methodology. Manual location of division blunders dependent on 278 video iris IMGand 360iris IMGedited from video face recordings brought about 0.316% of mistakenly sectioned from iris recordings and 0.717% inaccurately portioned IMGfrom face recordings (refer figure 8).

The impact of various iris improvement calculations on the general IR execution regarding the Equal Error Rates (EER) demonstrated in Table 3. These outcomes show that our calculation gives confirmation improvement of up to 6.17% in equivalent blunder rates over the first (unenhanced) iris IMGacknowledgment. The proposed calculation additionally shows preferred IMG upgrade over different calculations for up to 5% decrease in equivalent mistake rates. Specifically, the check execution of the proposed***l*-IEA** surpasses different adaptations of ***l*-IEA** upgrade application: unique***l*-IEA, *l*-IEA** with differentiation extending, veiling going before ***l*-IEA**.The outcomes likewise show the unfavorable impact of the foundation subtraction strategy on the EER due to enhancing the clamor in the difficult MBGC IMG. Figure 8 represents a reasonable DET bend to look at the impact of changed IMG upgrade calculations. Hence, the proposed 3-arrange ***l*-IEA**improves the presentation of iris confirmation by up to 5.3–7.15% regarding equivalent mistake rates.

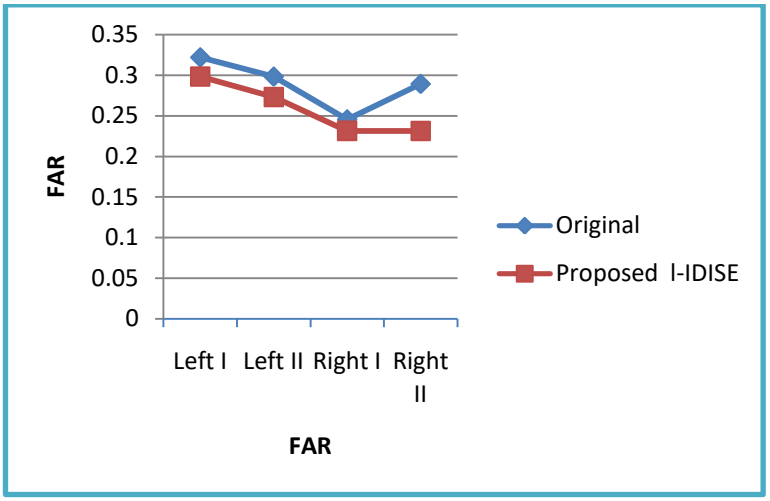

Figure. 8. Performance comparison for IR the original Vs. *l*-IDISE

5.4. BPANNMethod

The BPANN topology is a different layer comprising of 150 hubs for information, 3 hubs for covered up, and 1 hub for yield. It has 350 loads and predispositions to be put away in the database record. The information info stream is parallel for every iris IMG. By utilizing this system in the framework, execution time is around 35 seconds or less for iris IMG preparing because of the input word in BPANN learning calculation.

This BPANN topology achieved an acknowledgment rate of 90%. These rates are attributed to the tan-sigmoid exchange work, which is utilized in the yield layer. Table 4 shows tests for loads extricated from various iris designs. These loads might be utilized in IMG testing. At that point, the yield of BPANN checked to characterize the individual.

Table 4: BPANN Method Topology

Assessment	BPANN Method
Forward Flow	100 i/p - 1 o/p
Dataset	350
Rate of IR	91.13%
Error Tolerance	0.00010
Program Execution Speed	34 sec.

Image size	640x480

The Linear Associative Memory utilize just single layer organize yet in BPANN use multi-layer arrange, in LAM we have 100 information sources and one yield yet in BPANN we have 100 data sources layer 3 shrouded layers and one yield, the acknowledgment pace of BPANN is more than the Linear Associative Memory (LAM) for the iris tried IMG, the size of the IMGis same in the two systems. BPANN topology utilized is progressively precise. Next test, 200 IMGare taken. In the database, these IMGhave a place with 33 people. Every individual has 7 distinct IMG. The number of uproarious tried IMG that utilized in this trial was 99. Utilizing BPANN, 92 IMGwas perceived adequately with acknowledgment exactness 92.9%.The 300 IMGis taken in the next examination. These IMGhave a place with 40 people, and every individual has 8 unique IMG. The number of noisy tried IMGthat are utilized in this trial was 80. Utilizing BPNN, 75 IMGwas perceived effectively with acknowledgment precision 93.8% (refer table 5).

Table.5: Measurement for IR images

Comparison	IR Sample	BPANN – Right	BPANN – Left
25	40	92.16 %	7.97 %
35	90	93.14%	7.13%
50	75	98.14%	0.72%

The acknowledgment of irises is performed utilizing the BPANN. 500 man's IMGis chosen for the iris database for the characterization. The recognized irises after standardization and upgrades are scaled by utilizing averaging — this assistance to decrease the size of the BPANN. The IMGis spoken to by the networks. The lattices are the info signal for the BPANN. The yield of the BPANN is classes of iris design. For each arrangement of iris IMG, the two examples are utilized for the preparation, and the other two are utilized for the testing. The acknowledgment rate for the BPANN is 99.25%. In a similar time, the proposed framework utilizes from the IMG database of 500 man's IMGare taken, and everyone has four distinct IMG; two of them are utilized for the testing and the different pieces of proof. The calculation utilized for the proposed framework demonstrates the aftereffect of 99.50%.

6. Conclusion and Future work

In this paper, a methodology for IRS has been *l*-IDISE proposed. Straightforward morphological activities and 3D sifting procedures are utilized to identify the student. The commotions, for example, eyelashes, and reflections are expelled through the straight thresholding. The BPANN stage comprises of two stages: preparing the stage for human iris recognizing and testing stage for choosing whether the human iris exists on the database or not.

It is seen that the proposed methodology is progressively proficient for the considered dataset from the trial results. It is likewise seen that the proposed methodology sets aside sensible measures of effort to perform iris division, and acknowledgment exactness is additionally sensible. BPANN can be utilized for iris design arrangement, and it has points of interest in speed and exactness.This proposed another *l*-IDISE dependent on the use of the *l*-IEA to standardized iris IMG. It comprises of veiling of loud districts, the use of the first *l*-IEA, and the resulting differentiation extending. The proposed *l*-IEA calculation is reasonable for the upgrade of standardized iris IMG preceding component extraction. The outcomes demonstrate that the proposed upgrade calculation improves the check execution of up to 5-7.5% of iris IMG. In this way, the proposed iris IMG upgrade calculation has potential pertinence in IRS,mainly when speed is an issue.The future work is testing the effect on the exactness of the proposed methodology over a huge dataset and growing increasingly powerful IRS appropriate for genuine applications. Future research will incorporate the execution of the versatile choice of the ***l*-IEA** parameters. Also, neighborhood versatile iris IMG improvement will be created to lessen the distinction in light between different pieces of an iris IMG and testing the upgrade calculation on more information.

References

[1] R.P. Wildes "Iris Recognition: An Emerging Biometric Technology" Proc. IEEE vol. 85 no. 9 pp. 1348-1363 1997.

[2] J. Daugman. How iris recognition works. Proceedings of 2002 International Conference on Image Processing, Vol. 1, 2002.

[3] Wildes, R.P., Asmuth, J.C. et al., "A System for Automated Iris Recognition," Proc. of the Second IEEE Workshop on Applications of Computer Vision, 1994, pp.121-128.

[4] Jiali Cui, Yunhong Wang, JunZhou Huang, Tieniu Tan, and Zhenan Sun, "An Iris Image Synthesis Method Based on PCA and Super-resolution," IEEE CS Proceedings of the 17th International Conference on Pattern Recognition (ICPR'04).2004.

[5] J. R. Bergen, P. Anandan, K. Hanna, R. Hingorani, "Hierarchical model-based motion estimation," *Proc. Euro. Conf. Computer Vision*, pp. 5-10, 1991.

[6] F. Bouchier, J. S. Ahrens, G. Wells, *Laboratory evaluation of the IriScan prototype biometric identifier*, 1996.

[7] M. Adam, F. Rossant, B. Mikovicova, and F. Amiel, "Iris identification based on a local analysis of the iris texture." Proceedings of 6th International Symposium

November-December 2019
ISSN: 0193-4120 Page No. 5137 - 5145

on Image and Signal Processing and Analysis (ISPA 2009), Sept. 2009, 523-528.

[8] C. Belcher and Y. Du, "A selective feature information approach for iris image-quality measure." IEEE Transactions on Information Forensics and Security 3 (3), Sept. 2008, 572-577.30. R. Chen, X. Lin, T. Ding, and J. Ma, "Accurate and fast iris segmentation applied to the portable image capture device." IEEE International Workshop on Imaging Systems and Techniques (IST '09), May 2009, 80-84.

[9] R.D. Labati, V. Piuri, and F. Scotti, "Agent-based image iris segmentation and multiple views boundary refining." IEEE 3rd International Conference on Biometrics: Theory, Applications, and Systems (BTAS 09), Sept. 2009, 1-7.

[10] S V Sheela, P A Vijaya, "Iris Recognition Methods – Survey," International Journal of Computer Applications (0975 – 8887) Volume 3 – No.5, June 2010.

[11] 1Hugo Proença, Sílvio Filipe, Ricardo Santos, João Oliveira, Luís A. Alexandre, "The UBIRIS.v2: A Database of Visible Wavelength Iris Images Captured On-The-Move and At-A-Distance", IEEE Transactions on Pattern Analysis and Machine Intelligence, August2010, volume 32, page 1529-1535

[12] Zhenan Sun; Hui Zhang; Tieniu Tan; Jianyu Wang, "Iris Image Classification Based on Hierarchical Visual Codebook," Pattern Analysis and Machine Intelligence, IEEE Transactions on, vol.36, no.6, pp.1120,1133, June 2014

[13] Proenca, H.: Iris recognition: on the segmentation of degraded images acquired in the visible wavelength. IEEE Trans. Pattern Anal. Mach. Intell. 32(8) (2010

[14] Proenca, H.: Iris recognition: on the segmentation of degraded images acquired in the visible wavelength. IEEE Trans. Pattern Anal. Mach. Intell. 32(8) (2010

[15] Proenca, H.: Iris recognition: on the segmentation of degraded images acquired in the visible wavelength. IEEE Trans. Pattern Anal. Mach. Intell. 32(8) (2010)

[16] FascaGilgy Mary, P. Sunitha Kency Paul, J. Dheeba, "Human Identification Using Periocular Biometrics," International Journal of Science, Engineering and Technology Research (IJSETR) Vol. 2, No. 5, 2013.

[17] L. Ma, T. Tan, Y. Wang, and D.Zhang, "Efficient iris recognition by characterizing key local variations," IEEE Transactions on Image Processing. Vol. 13, pp.739–750, 2004.

[18] Usham Dias, Vinita Frietas, P. S. Sandeep, and Amanda Fernandes, "A Neural Network Based Iris Recognition System for Personal Identification," ICTACT Journal On Soft Computing, Vol. 1, No. 2, pp. 78-84, 2010.

[19] He, Z., Tan, T., Sun, Z., Qiu, X. "Robust eyelid, eyelash and shadow localization for iris recognition," In Proceedings of the International Conference on Image Processing, pp. 265–268,2008